JOURNAL OF VIROLOGY, Feb. 1992, p. 674–684
0022-538X/92/020674-11$02.00/0

Vol. 66, No. 2

The Requirement for a 5′ Stem-Loop Structure in Brome Mosaic Virus Replication Supports a New Model for Viral Positive-Strand RNA Initiation

GREGORY P. POGUE AND TIMOTHY C. HALL*

Department of Biology, Texas A&M University, College Station, Texas 77843-3258

Received 26 August 1991/Accepted 18 October 1991

Sequences with strong similarity to internal control regions 1 and 2 (ICR1 and -2; A and B boxes) of tRNA genes are found at the 5′ termini of the genomic RNAs of brome mosaic virus (BMV) and other plant viruses. The functionality of these motifs was studied by introducing point mutations into the ICR2-like sequence of pRNA-2 M/S, a BMV RNA-2 deletion mutant that replicates in the presence of RNAs-1 and -2 but does not encode a functional viral protein. The accumulation of positive-strand progeny from pRNAs bearing single and double base substitutions was 70 to 91% lower than that of the wild type, while the addition of single bases at position 8 of this motif reduced replication by 80%. These dramatic decreases in positive-strand synthesis paralleled decreases in transcription seen (C. Traboni, G. Ciliberto, and R. Cortese, Cell 36:179–187, 1984) from a $tRNA^{Pro}$ gene containing similar mutations, suggesting comparable functions for the ICR regions in protein factor binding and demonstrating that a wild-type composition of the virus ICR2-like motif is required for proper RNA replication. Substitutions introduced at bases surrounding the ICR2 motif yielded levels of pRNA replication that differed, depending on the maintenance of a putative 5′ stem-loop structure in the positive strand of the viral genome. Mutations disrupting this positive-strand stem-loop while maintaining the integrity of the complementary negative-strand structure reduced pRNA replication by 85 to 97%. In contrast, disruption of the negative-strand structure while maintaining the positive-strand stem-loop did not reduce pRNA replication. Similar positive-strand structures can be predicted to form from 5′ sequences of cucumber mosaic virus (strain Q) and cowpea chlorotic mottle virus RNAs-1 and -2, supporting the concept that such structures comprise an integral part of virus genomic positive-strand promoters. The requirement of a stem-loop structure present on the positive-strand provided the basis for a new model describing how these sequence and structural elements act in the production of virus positive-strand RNA.

The nonstructural proteins encoded by Sindbis virus and other alphavirus genomes show substantial amino acid homology with those of brome mosaic virus (BMV) and a wide range of plant viruses (2, 15). Such similarities suggest that, despite a diverse host range, these viruses share many aspects of replication strategy.

Studies on BMV, a tripartite positive-strand RNA virus of monocots, have led to the identification and functional characterization of several viral genomic sequences responsible for RNA replication (1, 10, 13, 31). The use of a template-dependent, template-specific replicase system in vitro defined sequences within the tRNA-like 3′ termini of BMV RNAs that promote negative-strand synthesis (8, 9). Additional studies in vivo using barley protoplasts and intact plants have confirmed the requirement for this region in promoter activity (6, 11, 39, 40). The core region and modulating elements of the BMV RNA-4 subgenomic promoter, present in the intercistronic region of RNA-3, were also defined initially by using in vitro approaches (26, 35) and subsequently extended by tests in vivo (14, 28). Although commonalities for negative-strand promotion by the tRNA-like 3′ termini of bromoviruses and the polyadenylated 3′ termini of the alphaviruses are not apparent, the subgenomic promoter regions of these viruses contain several blocks of sequence similarities (26) and functional parallels (24) with respect to subgenomic RNA production.

In contrast to the detailed knowledge summarized above for negative-strand and subgenomic promoters, but in common with the situation for almost all RNA viruses, the sequence elements responsible for genomic positive-strand RNA promotion of BMV are only now beginning to be elucidated. For example, the recognition that sequences at the 5′ termini of BMV RNAs (27) and several other virus genomes (29) show strong sequence similarity with internal control regions 1 and 2 (ICR1 and ICR2; A and B boxes) of tRNA gene promoters has provided an important stimulus for studies in this area (Fig. 1C). To examine the functionality of these tRNA promoter-like motifs, we introduced mutations of the ICR2-like region into pRNA-2 M/S, a deletion mutant of RNA-2 whose replication mimics that of a defective interfering RNA (38). This RNA is dependent on the *trans*-acting proteins provided by RNA-1 and -2 for its replication; because it does not contribute to viral functions, it was termed a parasitic RNA (pRNA). Base substitutions introduced at two positions of the 5′ ICR2-like motif of pRNA-2 M/S reduced replication by 82%, demonstrating the functionality of specific bases in virus replication. The effect on replication was shown to be primarily in positive-strand RNA synthesis by kinetic analysis of mutant and wild-type (wt) pRNA positive- and negative-strand accumulation (38). These and additional results provided sound evidence that the 5′ ICR-like elements constitute a vital element of the positive-strand promoter.

The involvement of 5′ sequences in virus replication has also been established for Sindbis virus (36). The deletion of

* Corresponding author.

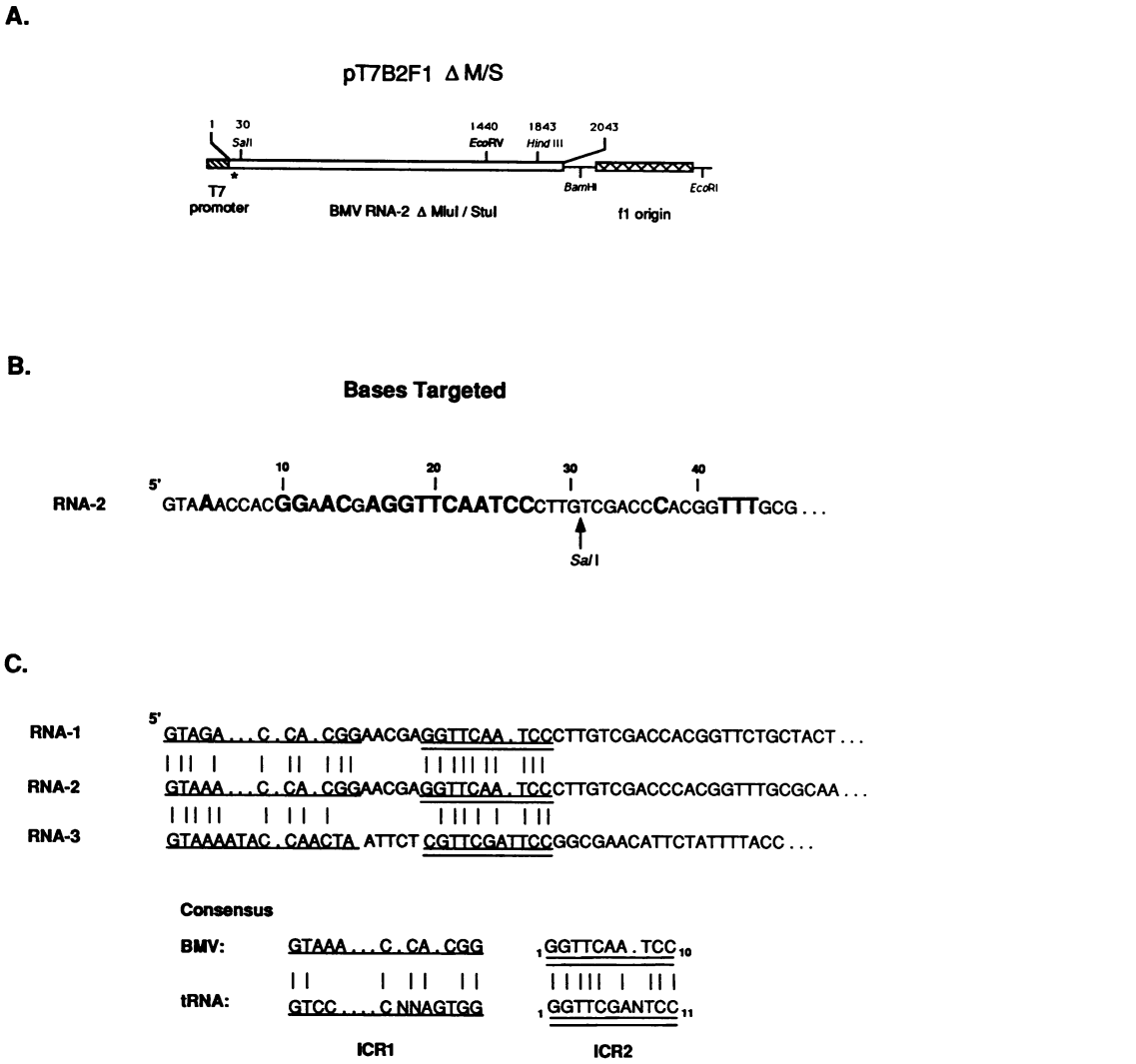

FIG. 1. Locations and sequences of the BMV ICR region and derived mutants. (A) Diagram showing transcriptional plasmid pT7B2F1 ΔM/S from which infectious pRNA-2 M/S and derivative mutants are transcribed. The ICR region is indicated (*), and the positions of the T7 promoter and the *Eco*RI-*Bam*HI fragment bearing the f1 origin, for ssDNA production, are denoted by diagonal hatching and cross-hatching, respectively. (B) 5′-Terminal bases of BMV RNA-2 and pRNA-2 M/S (derived from RNA-2 by internal deletion). The bases selected for mutagenesis within the positive-strand ICR-like region denoted by bold letters. The 5′ *Sal*I site is also indicated for orientation with respect to panel A. All sequences are given as in viral cDNA. (C) Comparison of 5′-terminal sequences of BMV RNA-1, -2, and -3 with the consensus ICR sequences of tRNA genes (according to reference 27). Spaces (.) are inserted to maximize apparent homology (|). Single and double underlines indicate ICR1-like (A box) and ICR2-like (B box) sequence motifs, respectively. The indicated numbers for the ICR2 (B box) sequences correspond to those used in the text. Because the variable (N_8) position of the tRNA motif is absent on BMV RNAs, the viral motif has 10 bases whereas the tRNA has 11.

specific bases in the 5′ terminus reduced virus accumulation to different levels, depending on the host cells used (mosquito or chicken), and it is likely that interactions with host-specific protein factors form the basis for the observed differences. A cloverleaf structure composed of the 5′-terminal 90 nucleotides (nt) of poliovirus positive-strand RNA has been shown experimentally to be required for virus replication and plaque formation (4). At least one protein of viral origin binds specifically to this structure, and mutations disrupting its ability to fold preferentially disrupt positive-strand RNA synthesis.

Because of the above reports on the involvement of 5′ structures in replication of animal viruses and our belief that ICR-like sequences are central to replication of BMV RNAs, we have undertaken an analysis of the structural and sequence requirements for positive-strand initiation, using the pRNA-2 M/S construct described previously (38). As will be shown, very poor replication resulted when base substitutions were introduced at each position within the ICR2-like motif, demonstrating its essential role in replication. Interestingly, mutations outside the ICR2 motif yielded differential efficacy in positive-strand synthesis, depending on the maintenance of a predicted 5′ stem-loop structure present in the positive-strand of the viral genome. As we now report, the results not only confirmed the requirement for tRNA promoter-like ICR sequences in the positive-strand pro-

moter of BMV but also provided an experimental basis for a new model describing how such sequences act in the production of virus positive-strand RNA.

MATERIALS AND METHODS

Chemicals and enzymes. Restriction and modifying enzymes were obtained from Boehringer Mannheim, New England Biolabs, and Bethesda Research Laboratories. T7 RNA polymerase and human placental RNase inhibitor (RNA Guard) were from Pharmacia. The cap analog m^7GpppG, T4 DNA ligase, and mung bean nuclease were from New England Biolabs.

Plasmid constructs. Full-length infectious RNA-1 and -2 were transcribed in vitro from cDNA clones pT7B1 and pT7B2 (11). The deletion mutant pT7B2 ΔM/S (Δ*Mlu*I/*Stu*I) was constructed (38) by deletion between *Mlu*I (base 1680) and *Stu*I (base 2502) sites of pT7B2. The f1 origin from pUC-f1 (Pharmacia) was inserted into pT7B2 ΔM/S as an *Eco*RI-*Bam*HI fragment, generating plasmid pT7B2F1 ΔM/S (Fig. 1A), to facilitate the production of single-stranded DNA (ssDNA) for in vitro mutagenesis. The RNA transcribed from this construct is referred to as pRNA-2 M/S.

Oligonucleotides and site-directed mutagenesis. Nucleotides within the 5′ terminus of pT7B2F1 ΔM/S altered by oligonucleotide site-directed mutagenesis are shown in Fig. 1B. Modifications of the Kunkel procedure (22) were used for mutagenesis of uracil-containing ssDNA as described previously (38). Oligonucleotides were synthesized to contain degenerate bases at the targeted position(s) in order to obtain an array of mutations. Sequential numbering has been used to define base substitutions within the ICR2-like motif. The eighth position of the ICR2 sequence in tRNA promoters is designated the N or variable base and is absent from the BMV motif. The $+X_{(8)}$ mutants (X representing any nucleotide) contain a single nucleotide insertion at the eighth position of the BMV ICR2-like motif. Mutations were also introduced in the ICR1-like domain (ICR1-XX), in the space between the ICR boxes (SBB) and downstream of the ICR2-like sequence (DS-X).

In vitro transcription and protoplast inoculation. Plasmids pT7B1, pT7B2, and pT7B2F1 ΔM/S and its mutant derivatives were linearized with *Bam*HI and used as templates for transcription. Capped full-length RNA transcripts were synthesized in vitro, using T7 RNA polymerase as described previously (11). Barley (*Hordeum vulgare* cv. Dickson; kindly provided by W. David Worrall, TAES-Vernon) leaf protoplasts were isolated (25) and inoculated with capped transcripts (separated from the DNA template by precipitation with 2.6 M LiCl) as described previously (39). Following transfection, protoplasts were incubated at room temperature under fluorescent lights for 24 h (unless specified otherwise), and RNA was extracted with sodium dodecyl sulfate-phenol and then ethanol precipitated (25).

Northern (RNA) blot analysis of progeny viral RNA. Viral progeny RNA from protoplasts were analyzed by Northern blots as described by Dreher et al. (11). Highly specific positive- and negative-sense ^{32}P-labeled RNA probes were transcribed from plasmid pT73TR, using either T3 or T7 RNA polymerase (39). This plasmid contains the cDNA corresponding to the tRNA-like structure (3′ terminal 200 bp) which is conserved among all BMV RNAs, including pRNA M/S and its mutant derivatives. The use of probes of equal length permitted direct molar comparison of positive- and negative-strand viral RNA levels.

Accumulation of progeny positive- and negative-strand RNA was measured from preflashed Northern autoradiographs (23), using a Bio-Rad model 620 video densitometer. The quantities of progeny pRNA M/S and derivative mutants were normalized with reference to RNA-1 levels, and the amount of the mutant RNA replicated was expressed as a percentage of the average replication level of wt pRNA-2 M/S.

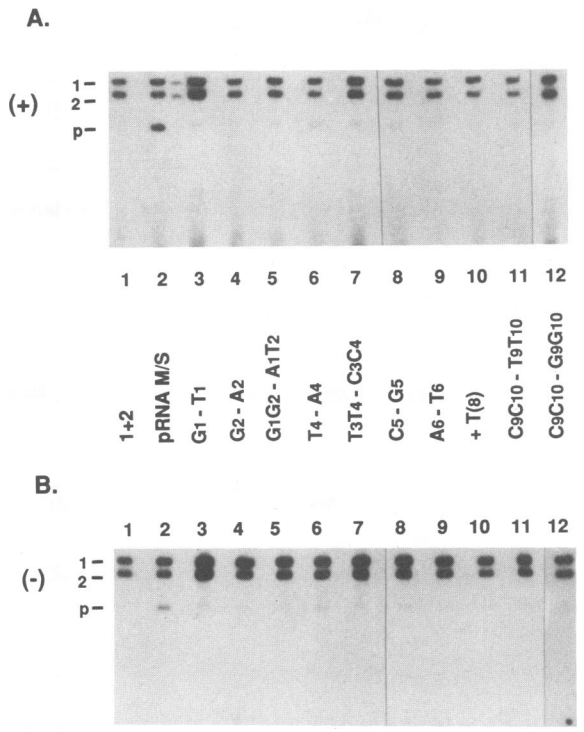

FIG. 2. RNA blot analysis of pRNA mutant replication characteristics in transfected barley protoplasts. Inocula contained transcripts (1 μg of each) of genomic RNA-1 and -2 plus the specified pRNA mutant. The name of each pRNA mutant added is indicated between the panels, and controls are shown in lanes 1 (no pRNA) and 2 (the parental pRNA-2 M/S). Positions of RNA-1 (1), RNA-2 (2), and the pRNA (p) are indicated at the left. Panels A and B show positive- and negative-strand progeny, respectively; panel B was exposed approximately twice as long as was panel A.

RESULTS

Nonstructural proteins expressed from RNA-1 and -2 (p1a and p2a, respectively) allow these RNAs to replicate in the absence of RNA-3 (13, 20, 40). However, reductions in the replication of these essential virus RNAs can deplete the amount of *trans*-acting protein, thereby decreasing the accumulation of all viral RNAs (39, 41). These reductions prevent accurate assessment of the *cis* effects of a given mutation on RNA replication. The use of an RNA component not contributing to viral functions but capable of replication as a vehicle for testing the replication and stability of mutant RNAs avoids these complications (38). The deletion mutant pRNA-2 M/S (2,043 nt) replicates at levels similar to those of RNA-1 (Fig. 2A, lane 2), providing an appropriate construct. For replication assays, protoplasts were inoculated with RNA-1 and -2 and the particular pRNA of interest. RNA-3 (2,117 nt) was omitted from these assays because its comigration on electrophoretic analysis with pRNA-2 M/S and its derivatives obscures their quantitation.

Although high levels of pRNA-2 M/S in the inoculum decrease accumulation of coinoculated BMV RNAs (32), the low levels (1 μg) of pRNA-2 M/S supplied in the inocula used in these studies caused only a slight decrease in replication of the parental RNA-2. No effect on RNA-1 was noted; therefore, it was used as an internal standard to control for any variations in infectivity of individual protoplast samples.

Mutations at all positions of the ICR2 motif debilitate replication. The 11-bp consensus ICR2 motif in tRNA genes, as compiled by Sharp et al. (44) and Sprinzl et al. (45), is GGTTCGANTCC (Fig. 1C). Over 90% conservation is seen for bases G_2, T_3, T_4, A_7, and C_{10}; some diversity is seen at positions G_1, G_6, and C_{11}, and position 9 is quite variable. The N_8 position is highly variable and sometimes missing in tRNA ICR2 sequences and is absent from the BMV motif (GGTTCAA.TCC; Fig. 1C). This absence displaces the numbering of the BMV motif by one and results in T_9 to C_{11} of the tRNA sequence being numbered as T_8 to C_{10} in the viral motif (Fig. 1C).

The ICR2 of $tRNA^{Pro}$ from *Caenorhabditis elegans* contains a sequence identical to the 5′ ICR2 motif in BMV RNA-1 and -2. Traboni et al. (46) used mutation analysis combined with evaluation of transcriptional activity in vivo to study the effects of modifications in the ICR2 motif of this gene. They found that although some variability was permissible at positions T_3 and A_7, each base analyzed was important. Since base conservation at a given position indicates that the site is of special importance (probably in binding of polymerase III or other protein factor), we thought it important to determine whether changes in sequence of the ICR2 motif in BMV RNA would functionally correspond to the effects seen for $tRNA^{Pro}$. Consequently, 30 mutations consisting of base substitutions or insertions within the ICR2-like sequence of pT7B2F1 ΔM/S were constructed, and the replication of the corresponding pRNAs was assayed in barley protoplasts 24 h postinoculation (p.i.). A Northern blot showing the replication characteristics of representative pRNA mutants is shown in Fig. 2, and a complete listing of the replication levels of all derived ICR2 mutants is included in Table 1. No mutant pRNA replicated at levels >30% of the wt level, demonstrating that single base substitutions within this conserved motif greatly reduce the suitability of these RNA templates for replication. The general pattern of replication showed more tolerance for substitutions in the center of the sequence motif, and the greatest freedom was seen at positions T_4, A_7, and T_8 (Table 1). It has been previously shown that mutations at positions A_7 and T_8 preferentially debilitate positive-strand synthesis early in infection, with negative-strand synthesis proceeding at wt rates (38). Such inhibition implies that positive-strand replication is primarily debilitated by mutations in the ICR2-like motif. Insertion of a single nucleotide at position 8 of the ICR2 sequence was not tolerated; insertional mutants pRNAs $+T_{(8)}$ (Fig. 2A, lane 10), $+A_{(8)}$, and $+C_{(8)}$ replicated at levels of 20% or less of the wt level (Table 1). Such intolerance for the insertion of bases within this motif emphasizes the tight conservation of sequences and a distinct requirement for the sequential order present in the wt sequence.

Mutant sequences show no increased susceptibility to degradation. To ensure that low accumulation levels of mutant pRNAs did not primarily result from preferential degradation, the stability of selected mutant pRNAs was compared with that of pRNA-2 M/S. Wild-type pRNA-2 M/S and a set of representative pRNAs with mutations spanning the ICR2-like motif were inoculated alone to barley protoplasts. Equal aliquots of cells were removed at 0, 4, 8, and 16 h p.i., and the RNA extracted from these protoplasts was analyzed by Northern blotting. Levels of residual input RNAs were normalized against the level of the particular pRNA at the 0-h time point (Fig. 3). No significant difference in stability was seen between ICR2-mutant pRNAs and the wt pRNA-2 M/S, indicating similar $t_{1/2}$ values (Fig. 3). Indeed, the degradation kinetics for wt pRNA-2 M/S were similar to those for pRNA C_5–G_5 up to 8 h p.i. (Fig. 3). Such results clearly demonstrate that mutations within the ICR2-like motif do not significantly alter RNA stability and that

TABLE 1. Positive-strand progeny accumulation of ICR2-mutant pRNAs[a]

pRNA	ICR2-like sequence	Relative pRNA level (%)
wt	GGTTCAATCC	100
G_1–T_1	TGTTCAATCC	17
G_2–T_2	GTTTCAATCC	15
G_2–A_2	GATTCAATCC	11
G_1G_2–T_1T_2	TTTTCAATCC	14
G_1G_2–T_1C_2	TCTTCAATCC	15
G_1G_2–A_1T_2	ATTTCAATCC	9
G_1G_2–A_1C_2	ACTTCAATCC	16
T_4–A_4	GGTACAATCC	25
T_3T_4–A_3A_4	GGAACAATCC	10
T_3T_4–A_3G_4	GGAGCAATCC	17
T_3T_4–C_3A_4	GGCACAATCC	14
T_3T_4–C_3C_4	GGCCCAATCC	12
T_3T_4–C_3G_4	GGCGCAATCC	12
T_3T_4–G_3C_4	GGGCCAATCC	14
C_5–A_5	GGTTAAATCC	21
C_5–G_5	GGTTGAATCC	16
A_6–C_6	GGTTCCATCC	15
A_6–T_6	GGTTCTATCC	14
A_7–G_7	GGTTCAGTCC	22
A_7–C_7	GGTTCACTCC	26
A_7–T_7	GGTTCATTCC	18
T_8–A_8	GGTTCAAACC	27
T_8–C_8	GGTTCAACCC	30
$+A_{(8)}$	GGTTCAAATCC	17
$+C_{(8)}$	GGTTCAACTCC	20
$+T_{(8)}$	GGTTCAATTCC	16
C_9C_{10}–T_9T_{10}	GGTTCAATTT	10
C_9C_{10}–A_9T_{10}	GGTTCAATAT	19
C_9C_{10}–G_9A_{10}	GGTTCAATGA	13
C_9C_{10}–G_9G_{10}	GGTTCAATGG	14

[a] Progeny positive-strand RNA was analyzed 24 h p.i. from barley protoplasts transfected with inocula containing BMV RNA-1 and -2 and pRNA-2 M/S or the specified derivative mutant. Following hybridization with a radioactive probe, the RNA blots were analyzed by densitometry (see Materials and Methods). The replication level for each pRNA was normalized with respect to that for RNA-1 and is expressed as a percentage of wt pRNA-2 M/S replication (100%). The value for each mutant pRNA represents the average of two to four independent experiments. The altered nucleotides (underlined) are numbered 1 to 10 with respect to their order in the ICR2-like motif (see Fig. 1C). The variable eighth (N_8) position of the ICR2 sequence in tRNA gene promoters is absent from the BMV motif (see text). The $+X_{(8)}$ mutants contain a single (designated) nucleotide inserted at the (N_8) position of the BMV ICR2-like sequence. The average standard deviation for the replication levels of all mutants tested in this study was 5.04, with 24 of the 35 mutant pRNAs having a deviation of 5 or less.

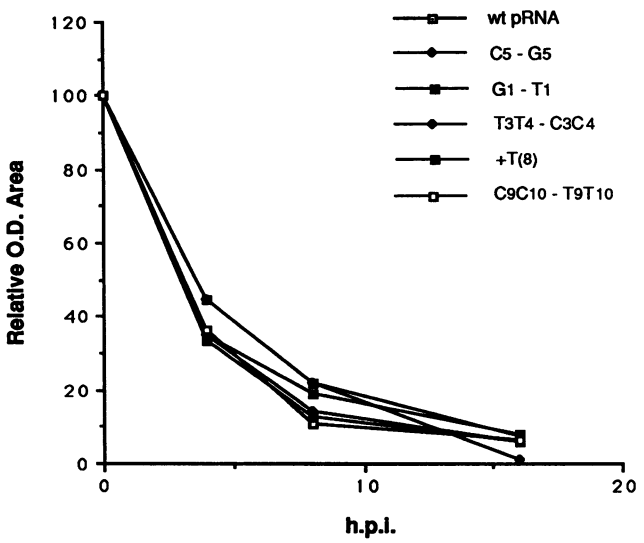

FIG. 3. Stability comparison of wt and mutant pRNAs. Barley protoplasts (10^6) were transfected with 3 μg of wt pRNA-2 M/S, C_5–G_5, G_1–T_1, T_3T_4–C_3C_4, $+T_{(8)}$, or C_9C_{10}–T_9T_{10} (in the absence of genomic RNA) and harvested at 0, 4, 8, and 16 h p.i. Total nucleic acid was extracted and analyzed by hybridization with ^{32}P-labeled negative-sense RNA probes corresponding to the conserved 3′ 200 nt of all BMV RNAs. The relative quantities of pRNA were obtained by quantitative densitometry and are expressed as a percentage of the level present at 0 h p.i.

reductions in accumulation truly reflect defects in RNA synthesis.

The presence of negative-strand RNA for each pRNA tested (Fig. 2B; 38) demonstrated that the positive-strand pRNAs seen in Fig. 2A do not represent exclusively the RNA supplied in the inoculum (input RNA). When the levels of pRNAs inoculated alone (Fig. 3) were compared with those obtained from inoculations that also contained RNA-1 and -2 (Fig. 2), very few new positive-strand RNAs could be detected. This result suggests that a substantial portion of the mutant pRNAs detected in Fig. 2A represent input positive-sense RNA which may have acted only as a template for initial rounds of negative-strand synthesis.

Evidence for a 5′ stem-loop in BMV positive-strand RNAs. The actual structural form in which the ICR-like sequences contribute to positive-strand promoter functions was not revealed by these experiments. Previously, we have shown that the 3′ end of BMV negative-strand RNA-1 can be predicted to fold into a structure resembling a methionine initiator tRNA ($tRNA^{Meti}$), with the TφC loop being especially well conserved (29). While the 3′ bases of negative-strand RNA-2 could form a similar but less stable structure, we have been unable to obtain similar folding for the 3′ terminus of RNA-3 negative strand. As found in the RNA-1 negative-strand structure, the putative TφC loop analog of the RNA-2 negative-sense structure contains a $tRNA^{Meti}$-like ICR2 sequence (38). This folding of the 44 terminal bases has a stability of $\Delta G = -12.9$ (7) (Fig. 4B). The complementary bases in the 5′ terminus of the positive strand can also be predicted to fold into a stem-loop structure of 46 bases in length and having a ΔG of −13.1 (Fig. 4A). The positive-strand structure consists of a terminal loop containing the ICR2-like sequence followed by a stem (a), a second loop region (b), and a second stem (c) extending to the 5′-terminal viral base, not including the methylated cap structure (Fig. 4A). Indeed, the 5′-terminal bases of positive-strand BMV RNA-1 and -3 can be predicted to fold into similar structures (Fig. 4A). Importantly, although the BMV RNAs contain a high degree of sequence similarity in part of this region, any sequence divergence between RNA-1, -2, and -3 in the extreme 5′ bases is compensated by appropriate base changes in the 3′ region of the ICR2-like motif, permitting conservation of structure.

Structural conservation in the midst of sequence divergence suggests a functional role for the 5′ stem-loop structures in the virus life cycle. To extend our knowledge as to which bases are necessary for viral replication and to evaluate which structure, positive or negative strand (if either), is required for promoter activity, G · U mutations were introduced into the 5′ end of pRNA-2 M/S to selectively disrupt either the positive- or negative-strand structure. Such G · U pairings maintain folding in one strand, while the complementary A · C base pairs of the opposite strand cannot form, thus disrupting a stem structure. Figure 5 shows the predicted stem-loop regions present at the 5′-terminal positive-strand and the complementary negative-strand structure, with the bases targeted for mutagenesis boxed in the wt sequence. The bases altered in each mutant sequence have been also boxed. Extensive computer modeling (7) was used to corroborate all predicted structures shown in Fig. 5.

Disruption of the 5′ stem-loop structure by mutations flanking the ICR2 motif decrease replication. Mutant pRNA ICR1-GG1, in which AA was substituted for GG (bases 10 and 11 of the virus RNA) at the end of the ICR1-like motif (Fig. 1C), replicated to only 5% of the wt level in barley protoplasts (Fig. 5). This mutation completely disrupted base pairing in the loop (b) region while leaving the complementary negative-strand structure intact through the formation of two G · U base pairs. A second mutation (DS-UUU) in which the UUU (bases 42 to 44) were replaced with CCC reduced pRNA replication by over 95%. Such substitutions disrupt stem (c) of the positive-strand stem-loop while maintaining the integrity of the complementary negative-strand stem. Substituting a G for the C (base 37) residue allows the small stem in loop (b) to be extended by one base in the positive-strand structure while displacing one base and reordering a stem in the complementary positive-strand structure. Indeed, this pRNA (DS-C1), which exhibited improved thermodynamic stability, replicated at greater than wt levels. Additional mutations, similar to DS-C1, which altered the folding of the negative-strand structure also showed enhanced replication efficiency (37). Such data (Fig. 5) suggest that the 5′ stem-loop structure predicted to form in the positive strand is required, and functions in viral replication, rather than the putative 3′ negative-strand structure.

Further evidence supporting the hypothesis that a positive-strand stem loop is vital to RNA replication was obtained by testing two mutations (ICR1-A1 and -A2) at the A (base 4), both of which disrupt the terminal stem of the negative-strand stem loop structure. ICR1-A1, which has a C substituted for this A, created a bulge in stem (c) of the positive-strand structure and replicated at only 15% of the wt level (Fig. 5). In contrast, pRNA ICR1-A2, which has a G substituted at this position, replicated at close to wt levels and left the positive-strand structure intact by G · U base pairing (Fig. 5). To test the importance of stem (a) in RNA replication, GUG was substituted for the wt sequence ACA (bases 13, 14, and 16; Fig. 1B), so that this stem was almost entirely comprised of G · U base pairs. This mutation (SBB; not shown in Fig. 5) led to a predicted bulging of this stem.

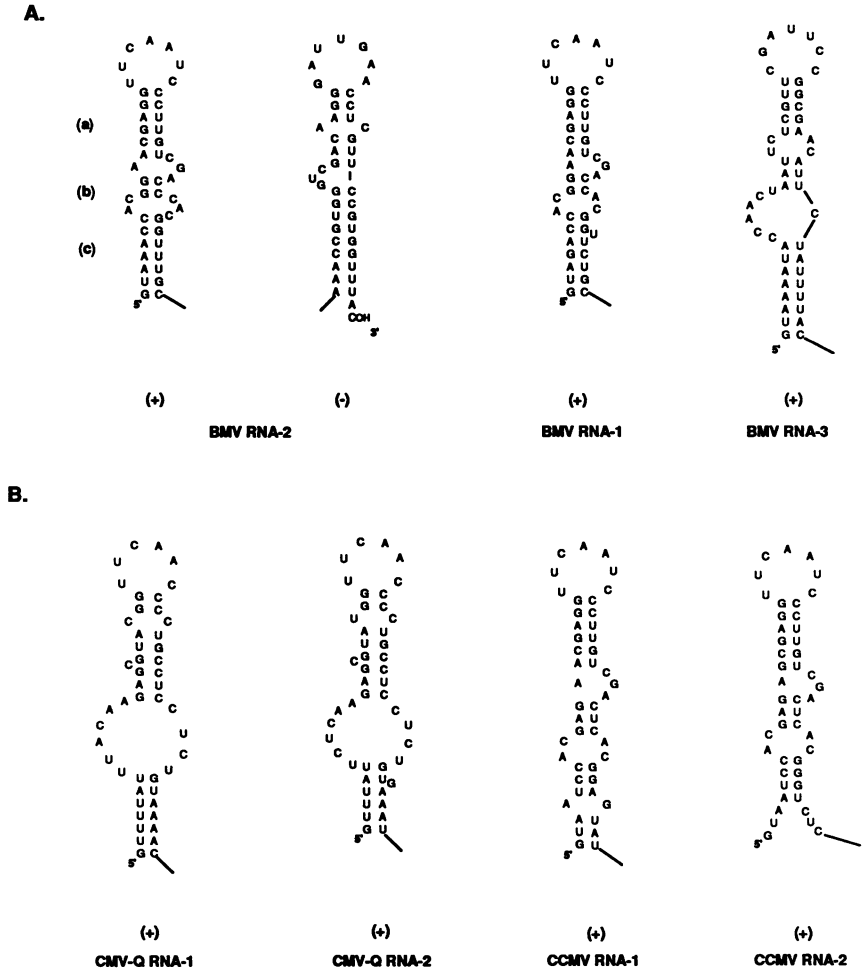

FIG. 4. Putative folding for 5′ positive-strand termini and 3′ negative-strand termini of RNAs from BMV and related viruses. As shown in panel A, a stable ($\Delta G = -13.1$) stem-loop can be formed by sequences present at the 5′-terminal region of BMV RNA-2 positive strand. Stems a and c and loop region b are indicated by bold letters. The complementary 3′ negative-strand terminus can also be folded to form a stem-loop ($\Delta G = -12.9$). Stem loop structures predicted for the 5′-terminal positive-strand sequences of BMV RNA-1 ($\Delta G = -12.5$) and RNA-3 ($\Delta G = -8.0$) are also shown in panel A. In panel B, the predicted stem-loop foldings for the 5′-terminal positive-strand sequences of other related viruses are shown: CMV (strain Q) (42, 43) RNA-1 ($\Delta G = -7.7$) and RNA-2 ($\Delta G = -4.1$) and CCMV (3) RNA-1 ($\Delta G = -11.4$) and RNA-2 ($\Delta G = -9.9$). Estimated structural stabilities of each RNA folding were derived by using the algorithm of Zucker as described elsewhere (7). In each stem-loop, the ICR2-like motif is present in the terminal loop region of each viral RNA.

However, the complementary folding of the region containing this mutation, though not identical to the folding of the wt, leads to a predicted negative-strand structure of greater stability than that of the wt. The pRNA bearing this mutation replicated at less than 5% of wt levels (37). When mutants ICR1-GG1, -A1, and -A2 were tested in tobacco protoplasts, replication levels similar to those seen in barley protoplasts were noted (37), supporting the notion that the putative positive-strand stem-loop structure functions in viral RNA replication. Since the pRNAs need not provide any translation products for replication, the participation of a positive-strand stem-loop (Fig. 4) in translation is expected to be minimal. The data presented in Fig. 4 and 5 show strong correlation between maintenance of the 5′ positive-strand stem-loop structure and the ability of pRNAs to replicate.

To provide a control for the possible introduction of second-site mutations during the mutagenesis reactions, a pRNA shown by sequencing of the untranslated 5′ region to be wt was tested for its ability to replicate in barley protoplasts. In multiple experiments, RNA transcribed from this clone accumulated at levels indistinguishable from those of wt pRNA-2 M/S, confirming that reductions in pRNA replication by 5′ mutations did not result from the acquisition of secondary mutations.

DISCUSSION

Functionality of ICR-like sequences in the replication of BMV positive strands. It has been proposed (27) that sequences resembling the internal promoters of tRNA genes, ICR1 and -2 (Fig. 1C), act as the core of the positive-strand genomic RNA promoter for BMV and other related tricornaviruses. Additional support for this novel concept was provided by the identification of ICR2-like sequences in a wide range of plant viruses (29). Convincing experimental evidence for the functionality of the ICR2-like sequence in positive-strand promotion has now been obtained (38), and the dramatic reductions in pRNA-2 M/S progeny resulting

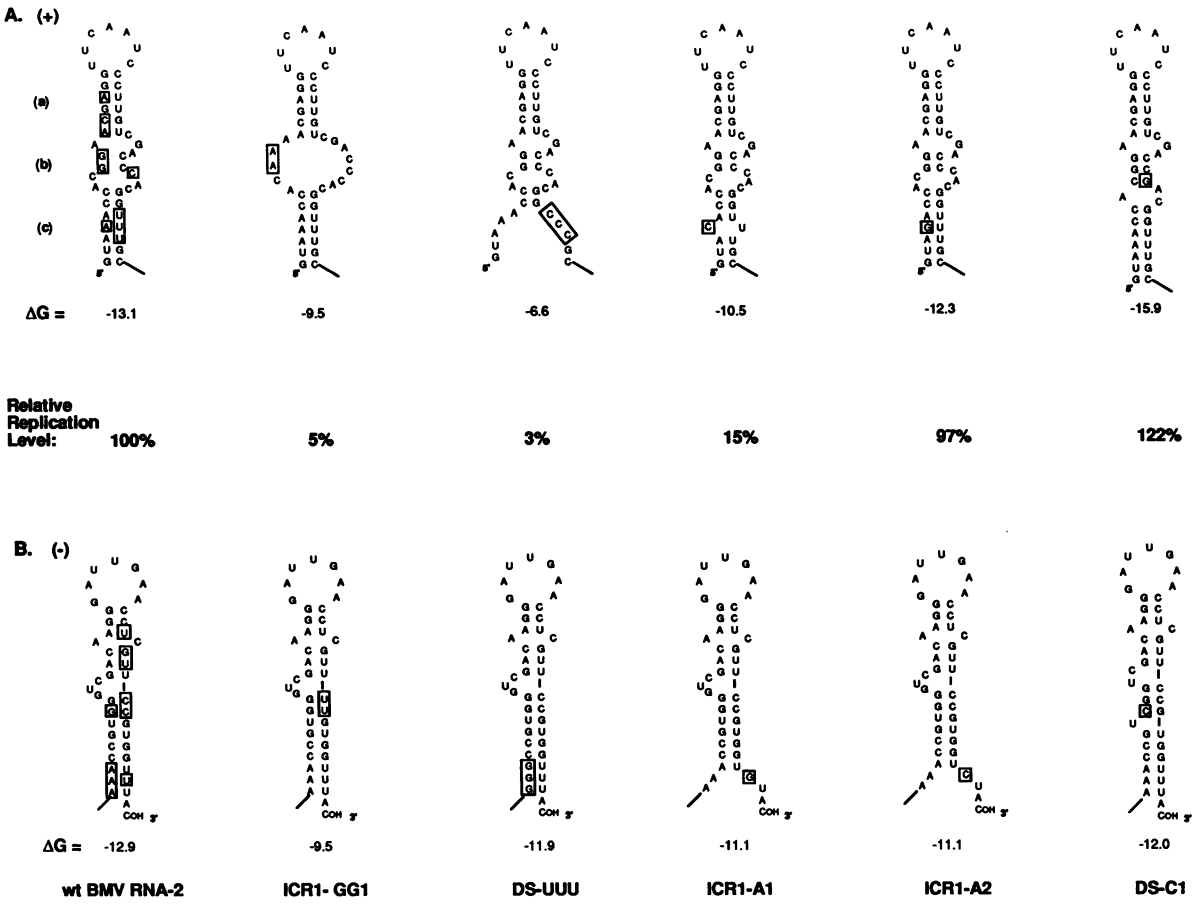

FIG. 5. Comparison of the predicted stem-loop structures present at the 5′ positive-strand terminus and the complementary 3′ negative-strand terminus of BMV RNA-2 and mutant derivatives obtained by site-directed mutagenesis. Bases selected for mutagenesis are boxed on the wt structures, and the sequence changes are boxed in the mutant structures. The predicted secondary structures for wt and mutant 5′ positive-strand termini are shown in panel A, and the corresponding negative-strand terminal structures are shown in panel B. The replication level (average of two independent experiments for which the average standard deviation of all mutants was less than 4), expressed as a percentage relative the progeny level (100%) for wt pRNA-2 M/S, and the structural stabilities for the mutants are shown between the panels. The name of each mutant is indicated below each pair of structures.

from single base substitutions within the ICR2-like motif documented in Fig. 2 and Table 1 rigorously establish its vital role in RNA replication. Importantly, preferential degradation of mutant pRNAs has been excluded as an explanation for reduced progeny from these constructs (Fig. 3).

Comparison of ICR2 sequences of the $tRNA^{Pro}$ gene (46) and the 5′ region of BMV RNA-2 shows them to be identical, even though $tRNA^{Pro}$ is transcribed by polymerase III from a DNA promoter and the BMV genome is RNA. The data presented here reveal that striking parallels also exist for the effect of sequence substitutions in the ICR2 regions of these genes on their function in vivo. For example, substitution of an A for T_4 reduces tRNA transcription by over 90% and pRNA replication by 75%. Other substitutions at this position, or double mutations including the adjacent T_3, result in even greater debilitation in both systems (46) (Table 1). Substitutions at A_7 reduced transcription of tRNAs by at least 77% and BMV replication by 74%. These similar values, coupled with the intolerance of the BMV motif to base additions (Table 1), indicate that the ICR2-like motifs in BMV RNAs may act analogously to ICR2 sequences in tRNA genes in binding a protein factor that is required for formation of the replication or transcription complex (19).

Mutations outside the BMV ICR2 motif which selectively disrupt the postulated positive-strand stem loop structure (Fig. 4) but maintain the integrity of the complementary negative-strand structure greatly reduced RNA replication (Fig. 5). In contrast, disruption of the putative negative-strand structure had little effect on pRNA replication (Fig. 5). These data resemble the requirement in poliovirus of a 90-nt cloverleaf structure present at the 5′ terminus of positive-strand RNA for viral infectivity (4). Mutations disrupting this structure selectively reduced the accumulation of positive-strand poliovirus RNA in vivo. These authors also found that incubation of the poliovirus cloverleaf RNA with extracts from infected cells resulted in the formation of two specific ribonucleoprotein complexes that involve both host and viral proteins.

Model for replication of virus positive strands based on the requirement for a 5′ positive-sense stem-loop structure. A requirement for stem-loop structures in the virus positive strand for synthesis of positive-strand RNA is unexpected, but the parallel occurrence of such structures in poliovirus and BMV supports the contention that they have a major function in RNA replication. Indeed, a coherent model for viral RNA replication that may be applicable to diverse virus

groups can be developed, based on a requirement for such positive-strand structures. It has been demonstrated (34) that the single-stranded 3′-CCA_{OH} terminus of the BMV positive-strand tRNA-like structure is the site of negative-strand RNA initiation (Fig. 6A). Although the nascent negative-strand product (Fig. 6B) is likely to be essentially double stranded, the addition of ssDNA or ssRNA fragments complementary to the 3′ terminus prevents the initiation of negative-strand synthesis in vitro (1). In contrast, fragments complementary to internal portions of the 3′ region were efficiently read through by the replicase complex (1). These results suggest that although replicase can separate lengthy internal double-stranded regions (presumably by a helicase function), a single-stranded terminus is mandatory for strand initiation. If a similar requirement for a single-stranded 3′ negative-strand terminus exists for the initiation of genomic positive strands, a mechanism must exist to release the 3′ negative-strand terminus from its (at least partially) double-stranded RNA form in the initial replicative-form positive- or negative-strand RNA product. As shown in Fig. 6B and C, the 5′-terminal positive-strand sequences analyzed in this study are postulated to act at this step. A soluble protein factor may recognize a portion of these sequences (Fig. 6B and C), inducing the formation or stabilization of the 5′ stem-loop structure shown in Fig. 6C. Since mutations of the well-conserved ICR2-like motif cause dramatic decreases in replication with little or no predicted disruption in secondary structure, the motif appears to be an excellent candidate for primary recognition by a binding protein. The identity of this putative protein factor is unknown, but the pivotal role of the ICR2 sequence makes a host polymerase III transcription factor(s) a very attractive candidate. However, a p1a helicase-like protein, elongation factors, or other proteins are possible alternative or additional candidates (5, 38).

The ability of the BMV replicase to read regions containing complex double-stranded RNA and regions containing very stable RNA-DNA hybrids (1) provides evidence favoring the involvement of the p1a helicase-like protein in the replication complex (17). Protein p1a possesses significant amino acid homology with the 126-kDa protein of tobacco mosaic virus and nsP1 of Sindbis virus, which have been shown to possess activities associated with mRNA capping functions, guanylyltransferase (12) and methyltransferase (33), respectively. Such homology data strongly suggest a role for p1a in the capping of newly synthesized positive-strand RNAs. The p1a polypeptide may remain anchored at the 3′ terminus of the negative-strand template or become associated with the nascent positive strand (Fig. 6D). It is conceivable that two p1a polypeptides are present, one remaining as an anchor (perhaps to a nuclear or other membrane as well as functioning in capping) and the other providing the helicase function of the new positive-strand replicase complex (Fig. 6D).

Binding of the host protein factor to the ICR2-like motif (Fig. 6B) is postulated to elicit folding of the 5′-terminal stem loop as a hinge (Fig. 6C), thereby releasing a single-stranded 3′ negative-strand terminus for replicase recognition. As shown in Fig. 6D, the positive-strand replicase complex then recognizes this structure and initiates genomic positive-strand synthesis, using the negative-sense RNA as its template. Once synthesis begins, the absence of the replicase complex may elicit the soluble protein factor to dissociate from the stem-loop structure and bind the ICR2-like sequence of the newly synthesized positive-strand RNA to mediate initiation of the next positive strand (Fig. 6E and F).

This model permits multiple positive strands to be synthesized from each negative-strand RNA template but restricts the initial negative strand from leaving the replication cycle (Fig. 6C to F). Such a closed system may be responsible for the difficulty in obtaining protein extracts from infected tissue which will accept exogenously supplied template for positive-strand synthesis (16). Rao and Hall (40) showed that only catalytic amounts of p2a, the putative core polymerase (18), are required for BMV replication. These studies made it clear that each p2a molecule can reinitiate on multiple positive- or negative-strand templates. In contrast, continuous translation of p1a appears to be required in vivo for the amplification of BMV RNAs (41), suggesting that much greater quantities of this protein than of p2a are required. This view is consistent with the postulated multifunctional nature of the p1a protein (21) and the model presented in Fig. 6.

Relevance of the model to positive- and negative-strand asymmetry in BMV replication. Replication of BMV RNA proceeds in a highly asymmetric manner, 100 positive strands being produced for every negative strand (28). This property is shared by poliovirus, which replicates at a 20:1 to 30:1 positive-/negative-strand ratio (4). Indeed, any model of positive-strand replication must provide a mechanism for the asymmetric replication seen for all positive-strand RNA viruses studied. However, a close interdependence between positive- and negative-strand synthesis exists for BMV replication. This is evidenced by the fact that mutations within the tRNA-like structure, which were shown in vitro to be debilitated in negative-strand promoter activity (9), yielded low levels of positive-strand RNA progeny in vivo (11). Similarly, mutations within the 5′ ICR2-like sequence of pRNA-2 M/S selectively reduce positive-strand synthesis only early in infection, with negative-strand synthesis (Fig. 2B) decreasing at later time points (not shown here), as reported previously (38).

The close interdependence of positive- and negative-strand synthesis in BMV replication can be explained by the model presented in Fig. 6, which predicts that RNAs bearing mutations in the 5′ terminus of the RNA would give rise to low levels of both positive- and negative-strand RNA progeny. For example, mutations affecting the ICR2 motif (Table 1) or the structural integrity of the 5′ stem-loop structure (Fig. 5) are likely to debilitate the release of the postulated single-stranded 3′ terminus (Fig. 6C), making this a rate-limiting step in the initiation of positive-strand synthesis. Further, either type of mutation would disfavor recognition of the hinge structure by the replicase and slow or halt production of new positive strands. Reduced negative-strand synthesis from such mutants also occurs, since kinetic data for progeny accumulation show that once replication has commenced, newly replicated positive-strand RNAs provide the vast majority of templates for new negative-strand synthesis (38). In consequence, reduced levels of negative-strand accumulation will reflect the lowered availability of suitable positive-strand templates.

Predicted positive-sense stem-loop structures in other RNA virus groups. The functionality of positive-strand 5′ stem structures in viral replication and the correctness of the model described above are supported by the ability to derive structures similar to those postulated for BMV RNA for the 5′ termini of RNA-1 and -2 of cucumber mosaic virus CMV (Q strain) and cowpea chlorotic mottle virus (CCMV) (Fig. 4B). Attempts to obtain similar folding patterns for these viruses from their complementary 3′ negative-strand RNA sequences have been unsuccessful. The 5′ positive stem-loops of BMV, CMV, and CCMV have ΔG values ranging

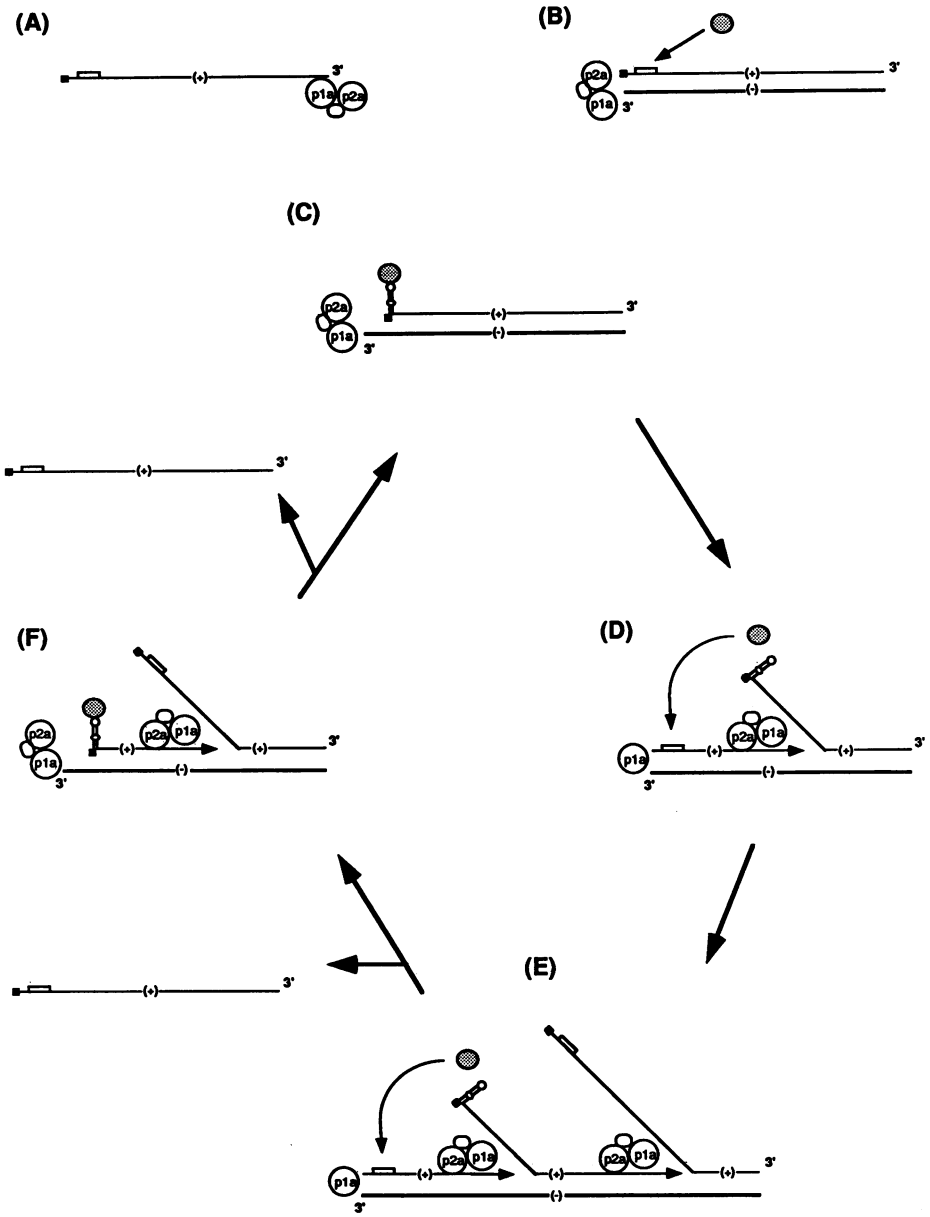

FIG. 6. Model for genomic positive-strand RNA synthesis. (A) Following translation, virally encoded nonstructural peptides p1a and p2a (circled) are thought to associate with a host factor(s) (small unlabeled oval) to form the viral negative-strand replicase complex that recognizes the 3′ end of the positive-strand inoculum RNA (thin line with the 5′ cap shown as a small filled box and the ICR motif denoted as an open box) and initiates synthesis of the negative strand. (B) Following completion of complementary negative-strand RNA (thick line) synthesis, the replicase remains associated with the terminal region of the partially double-stranded replicative form of viral RNA. A host protein (stippled circle), possibly a polymerase III transcription factor, is shown binding to the positive-strand ICR motif, eliciting (C) bending at the ICR motif hinge to form a characteristic stem-loop structure (see Fig. 4 and 5) from the 5′-terminal sequences. (D) The hinge structure is recognized by the negative-strand replicase which (putatively) associates with the host factor bound to the positive strand to become a positive-strand replicase, and new positive-strand synthesis initiates opposite the single-stranded 3′ terminus of the negative strand. One molecule of p1a may remain associated with the terminus of the viral RNA and participate in capping the newly synthesized positive strand. A second p1a molecule may associate with p2a and facilitate separation of RNA strands through its helicase function. (E) Once new positive-strand replication has begun, the protein (transcription) factor dissociates from the stem-loop structure of the original positive strand and binds to the ICR-like region of the newly synthesized positive strand, again inducing the formation of the hinge structure. Binding of additional viral replicase peptides to the hinge structure allows the synthesis of multiple positive strands from one negative-strand template. A situation similar to that presented in panel E probably represents the steady state in genomic RNA synthesis. (F) Once the original positive strand is released (denoted by exit [arrow]), the replicase binds to the new positive-strand hinge complex and a further round of genomic positive-strand synthesis is initiated.

from −4 to −13 (Fig. 4), and binding of a protein factor (Fig. 6) may contribute additional stabilization. The only sequence held in common between these viral structures is ICR2-like motif, which forms the central loop of each structure (Fig. 4). In each case, sequence divergences in the regions 3′ of the ICR2-like motifs are compensated for by base differences in the extreme 5′-terminal region. Except for CCMV RNA-2, stem (c) extends to the 5′-terminal G residues of each viral structure (Fig. 4). The conservation of such similar structures amid extensive sequence divergence supports the concept that they are required sequence elements.

Contribution of internal sequences to BMV replication. While the data presented here reveal that the stem-loop structure at the 5′ terminus of the genomic positive strands represents the primary element directing positive-strand replication, much evidence exists showing that other sequence and structural elements may be essential to viral replication. In addition to the sequence and structural elements of the positive-strand promoter at the 3′ end of the genomic RNAs, internal regions have been shown to modulate replication.

In the case of BMV RNA-2, deletion mutants lacking sequences corresponding to the N-terminal portion of the p2a cistron have been shown to produce no positive-strand RNA progeny (47). However, since no evidence for negative-strand progeny was provided for these mutants, their primary lesion may be in negative- rather than positive-strand synthesis. Indeed, certain deletion mutants of RNA-2 lacking sequences 5′ of base 1440 (within the p2a cistron) are incapable of producing negative-strand progeny (32). Such evidence shows that caution must be exercised in drawing conclusions regarding the effects of large sequence deletions, which frequently result in unpredictable alterations in overall RNA structure, yielding pleiotropic effects on biological activity.

Functional analysis in vivo of BMV RNA-3 deletion mutants defined a region between its two cistrons as being primarily responsible for amplification (13). Several ICR2-like sequence elements lie within this intercistronic region (27), and deletion of one of these internal ICR2 motifs has been found to reduce RNA-3 replication by over 80% (30). Clearly, the internal regions of BMV RNA-3 are major elements for positive-strand replication. The complexity of this RNA, which also generates positive-strand subgenomic RNA-4, probably contributes to difficulties in a mechanistic interpretation of its role in genomic positive-strand replication within the model presented in Fig. 6. Structural analysis of viral RNA in solution, combined with protein binding studies, will help to clarify the situation in regard to RNA-3 and to verify the existence and functionality of the 5′ stem-loop structures described here.

Conclusions. The results from this study rigorously demonstrate that the ICR2 motif present at the 5′ end of BMV RNA-2 is required in a sequence-specific manner for positive-strand RNA replication (Fig. 2; Table 1). Indeed, the importance of 5′ stem-loop structures in virus replication is strongly supported by the following observations: (i) bases surrounding the BMV ICR2 motif function in a structural capacity (Fig. 1B and 5); (ii) mutations selectively destabilizing the positive-strand stem loop structure greatly reduce viral replication (Fig. 5); (iii) stem loop structures can be predicted to form at the 5′ ends of several viral RNA positive strands (Fig. 4), indicating that such structures are conserved amid substantial sequence divergence; and (iv) insightful studies of poliovirus (4) have demonstrated that a cloverleaf structure present at the 5′ terminus of the viral RNA strand is required for positive-strand replication and the formation of ribonucleoprotein complexes with significance in replication. The model presented in Fig. 6 accommodates most characteristics known for virus replication and provides a plausible functional mechanism for 5′ strand stem-loop structures in positive-strand replication.

ACKNOWLEDGMENTS

We thank Loren Marsh for helpful discussions and Jim Carrington, María Restrepo-Hartwig, and Jim Connell for suggestions and critical review of the manuscript.

These studies were supported by NSF grant DMB-8921023 and fellowships (to G.P.P.) from W. R. Grace & Co. and the ARCS Foundation Inc.

REFERENCES

1. **Ahlquist, P., J. J. Bujarski, P. Kaesberg, and T. C. Hall.** 1984. Localization of the replicase recognition site within brome mosaic virus RNA by hybrid-arrested replication. Plant Mol. Biol. **3**:37–44.
2. **Ahlquist, P., E. Strauss, C. Rice, J. Strauss, J. Haseloff, and D. Zimmern.** 1985. Sindbis virus proteins nsp1 and nsP2 contain homology to nonstructural proteins from several RNA plant viruses. J. Virol. **53**:536–542.
3. **Allison, R. F., M. Janda, and P. Ahlquist.** 1989. Sequence of cowpea chlorotic mottle virus RNAs 2 and 3 and evidence of a recombination event during bromovirus evolution. Virology **172**:321–330.
4. **Andino, R., G. E. Rieckhof, and D. Baltimore.** 1990. A functional ribonucleoprotein complex forms around the 5′ end of poliovirus RNA. Cell **63**:369–380.
5. **Bastin, M., and T. C. Hall.** 1976. Interaction of elongation factor 1 with aminoacylated brome mosaic virus and tRNAs. J. Virol. **20**:117–122.
6. **Bujarski, J. J., P. Ahlquist, T. C. Hall, T. W. Dreher, and P. Kaesberg.** 1986. Modulation of replication, aminoacylation and adenylation in vitro and infectivity in vivo of BMV RNAs containing deletions within the multifunctional 3′ end. EMBO J. **5**:1769–1774.
7. **Devereux, J., P. Haeberli, and O. Smithies.** 1984. A comprehensive set of sequence analysis programs for the VAX. Nucleic Acids Res. **12**:387–395.
8. **Dreher, T. W., J. J. Bujarski, and T. C. Hall.** 1984. Mutant viral RNAs synthesized in vitro show altered aminoacylation and replicase template activities. Nature (London) **311**:171–175.
9. **Dreher, T. W., and T. C. Hall.** 1988. Mutational analysis of the sequence and structural requirements in brome mosaic virus RNA for minus strand promoter activity. J. Mol. Biol. **201**:31–40.
10. **Dreher, T. W., and T. C. Hall.** 1988. Replication of BMV and related viruses, p. 91–113. *In* E. Domingo, J. J. Holland, and P. Ahlquist (ed.), RNA genetics, vol. 1. CRC Press, Inc., Boca Raton, Fla.
11. **Dreher, T. W., A. L. N. Rao, and T. C. Hall.** 1989. Replication in vivo of mutant brome mosaic virus RNAs defective in aminoacylation. J. Mol. Biol. **206**:425–438.
12. **Dunnigan, D. D., and M. Zaitlin.** 1990. Capping of tobacco mosaic virus RNA—analysis of viral-coded guanylyltransferase-like activity. J. Biol. Chem. **265**:7779–7786.
13. **French, R., and P. Ahlquist.** 1987. Intercistronic as well as terminal sequences are required for efficient amplification of brome mosaic virus RNA3. J. Virol. **61**:1457–1465.
14. **French, R., and P. Ahlquist.** 1988. Characterization and engineering of sequences controlling in vivo synthesis of brome mosaic virus subgenomic RNA. J. Virol. **62**:2411–2420.
15. **Haseloff, J., P. Goelet, D. Zimmern, P. Ahlquist, R. Dasgupta, and P. Kaesberg.** 1984. Striking similarities in amino acid sequence among nonstructural proteins encoded by RNA viruses that have dissimilar genomic organization. Proc. Natl. Acad. Sci. USA **81**:4358–4362.

16. **Hayes, R. J., and K. W. Buck.** 1990. Complete replication of a eukaryotic virus RNA in vitro by a purified RNA-dependent RNA polymerase. Cell **63**:363–368.
17. **Hodgeman, T. C.** 1988. A new superfamily of replicative proteins. Nature (London) **333**:22–23.
18. **Kamer, G., and P. Argos.** 1984. Primary structural comparison of RNA-dependent polymerases from plant, animal and bacterial viruses. Nucleic Acids Res. **12**:7269–7282.
19. **Kassavetis, G. A., B. R. Braun, L. H. Nguyen, and E. P. Geiduschek.** 1990. *S. cerevisiae* TFIIIB is the transcription initiation factor proper of RNA polymerase III, while TFIIIA and TFIIIC are assembly factors. Cell **60**:235–245.
20. **Kiberstis, P. A., L. S. Loesch-Fries, and T. C. Hall.** 1981. Viral protein synthesis in barley protoplasts inoculated with native and fractionated brome mosaic virus RNA. Virology **112**:804–808.
21. **Kroner, P. A., B. M. Young, and P. Ahlquist.** 1990. Analysis of the role of brome mosaic virus 1a protein domains in RNA replication, using linker insertion mutagenesis. J. Virol. **64**: 6110–6120.
22. **Kunkel, T. A.** 1985. Rapid and efficient site-specific mutagenesis without phenotypic selection. Proc. Natl. Acad. Sci. USA **82**:488–492.
23. **Laskey, R. A., and A. D. Mills.** 1977. Enhanced autoradiographic detection of ^{32}P and ^{125}I using intensifying screens and hypersensitized film. FEBS Lett. **82**:314–316.
24. **Levis, R., S. Schlesinger, and H. V. Huang.** 1990. Promoter for Sindbis virus RNA-dependent subgenomic RNA transcription. J. Virol. **64**:1726–1733.
25. **Loesch-Fries, L. S., and T. C. Hall.** 1980. Synthesis, accumulation and encapsidation of individual brome mosaic virus RNA components in barley protoplasts. J. Gen. Virol. **47**:323–332.
26. **Marsh, L. E., T. W. Dreher, and T. C. Hall.** 1988. Mutational analysis of the core and modulator sequences of the BMV RNA3 subgenomic promoter. Nucleic Acids Res. **16**:981–995.
27. **Marsh, L. E., and T. C. Hall.** 1987. Evidence implicating a tRNA heritage for the promoters of (+) strand RNA synthesis in brome mosaic virus and related viruses. Cold Spring Harbor Symp. Quant. Biol. **52**:331–341.
28. **Marsh, L. E., C. C. Huntley, G. P. Pogue, J. P. Connell, and T. C. Hall.** 1991. Regulation of (+):(−) strand asymmetry in brome mosaic virus RNA. Virology **182**:152–160.
29. **Marsh, L. E., G. P. Pogue, and T. C. Hall.** 1989. Similarities among plant virus (+) and (−) RNA termini imply a common ancestry with promoters of eukaryotic tRNAs. Virology **172**: 415–427.
30. **Marsh, L. E., G. P. Pogue, and T. C. Hall.** Unpublished data.
31. **Marsh, L. E., G. P. Pogue, C. C. Huntley, and T. C. Hall.** 1991. Insight into replication strategies and evolution of (+) strand RNA viruses provided by brome mosaic virus. Oxford Surv. Plant Mol. Cell Biol. **7**:297–334.
32. **Marsh, L. E., G. P. Pogue, U. Szybiak, J. P. Connell, and T. C. Hall.** 1991. Non-replicating deletion mutations of BMV RNA-2 interfere with viral replication. J. Gen. Virol. **72**:2367–2374.
33. **Mi, S., R. Durbin, H. V. Huang, C. M. Rice, and V. Stollar.** 1989. Association of the Sindbis virus RNA methyltransferase activity with the nonstructural protein nsp1. Virology **170**:385–391.
34. **Miller, W. A., J. J. Bujarski, T. W. Dreher, and T. C. Hall.** 1986. Minus-strand initiation by brome mosaic virus replicase within the 3′ tRNA-like structure of native and modified RNA templates. J. Mol. Biol. **187**:537–546.
35. **Miller, W. A., T. W. Dreher, and T. C. Hall.** 1985. Synthesis of brome mosaic virus subgenomic RNA in vitro by internal initiation on (−) sense genomic RNA. Nature (London) **313**:68–70.
36. **Nesters, H. G. M., and J. H. Strauss.** 1990. Defined mutations in the 5′ nontranslated sequence of Sindbis virus RNA. J. Virol. **64**:4162–4168.
37. **Pogue, G. P., and T. C. Hall.** Unpublished data.
38. **Pogue, G. P., L. E. Marsh, and T. C. Hall.** 1990. Point mutations in the ICR2 motif of brome mosaic virus RNAs debilitate (+)-strand replication. Virology **178**:152–160.
39. **Rao, A. L. N., T. W. Dreher, L. E. Marsh, and T. C. Hall.** 1989. Telomeric function of the tRNA-like structure of brome mosaic virus RNA. Proc. Natl. Acad. Sci. USA **86**:5335–5339.
40. **Rao, A. L. N., and T. C. Hall.** 1990. Requirement of a viral *trans*-acting factor encoded in brome mosaic virus RNA-2 provides strong selection in vivo for functional recombinants. J. Virol. **64**:2437–2441.
41. **Rao, A. L. N., C. C. Huntley, L. E. Marsh, and T. C. Hall.** 1990. Analysis of RNA stability and (−) strand content in viral infections using biotinylated RNA probes. J. Virol. Methods **30**:239–250.
42. **Rezaian, M. A., R. H. V. Williams, K. H. J. Gordon, A. R. Gould, and R. H. Symons.** 1984. Nucleotide sequence of cucumber mosaic RNA 2 reveals a translation product significantly homologous to corresponding proteins of other viruses. Eur. J. Biochem. **143**:277–284.
43. **Rezaian, M. A., R. H. V. Williams, and R. H. Symons.** 1985. Nucleotide sequence of cucumber mosaic virus RNA1: presence of a sequence complementary to part of the viral satellite RNA and homology with other viral RNAs. Eur. J. Biochem. **150**:331–339.
44. **Sharp, S. J., J. Shaack, L. Cooley, D. J. Burke, and D. Söll.** 1985. Structure and transcription of eucaryotic tRNA genes. Crit. Rev. Biochem. **19**:107–144.
45. **Sprinzl, M., T. Hartmann, J. Weber, J. Blank, and R. Zeidler.** 1989. Compilation of tRNA sequences and sequences of tRNA genes. Nucleic Acids Res. **17**:1–173.
46. **Traboni, C., G. Ciliberto, and R. Cortese.** 1984. Mutations in box B of the promoter of a eukaryotic $tRNA^{Pro}$ gene affect rate of transcription, processing, and stability of the transcripts. Cell **36**:179–187.
47. **Traynor, P., B. M. Young, and P. Ahlquist.** 1991. Deletion analysis of brome mosaic virus 2a protein: effects on RNA replication and systemic spread. J. Virol. **65**:2807–2815.